RSC Advances

COMMUNICATION

View Article Online
View Journal | View Issue

Cite this: RSC Adv., 2015, 5, 106083

Received 1st October 2015
Accepted 3rd December 2015

DOI: 10.1039/c5ra20289b

www.rsc.org/advances

Published on 07 December 2015. Downloaded on 3/2/2020 4:50:36 AM.

Thermoresistive properties of p-type 3C–SiC nanoscale thin films for high-temperature MEMS thermal-based sensors†

Toan Dinh,‡*[a] Hoang-Phuong Phan,‡[a] Takahiro Kozeki,[b] Afzaal Qamar,[a] Takahiro Namazu,[b] Nam-Trung Nguyen[a] and Dzung Viet Dao[ac]

We report for the first time the thermoresistive property of p-type single crystalline 3C–SiC (p-3C–SiC), which was epitaxially grown on a silicon (Si) wafer, and then transferred to a glass substrate using a Focused Ion Beam (FIB) technique. A negative and relatively large temperature coefficient of resistance (TCR) up to −5500 ppm K^{-1} was observed. This TCR is attributed to two activation energy thresholds of 45 meV and 52 meV, corresponding to temperatures below and above 450 K, respectively, and a small reduction of hole mobility with increasing temperature. The large TCR indicates the suitability of p-3C–SiC for thermal-based sensors working in high-temperature environments.

In recent years, silicon carbide (SiC) has emerged as an appropriate material for high-temperature electronics thanks to its superior properties, such as large band gap and high thermal conductivity.[1–4] To date, more than 200 SiC polytypes such as 3C, 4H and 6H have been discovered.[5,6] Among these polytypes, single crystalline 3C–SiC, with its capability of being grown on a large-diameter silicon (Si) wafer (*e.g.* 300 mm), is one of the main technological polytypes.[7–9] Thanks to its high temperature coefficient of resistance (TCR),[10] large band gap[11] and fast thermal response,[12] 3C–SiC would be a good material for developing thermal sensors such as temperature sensors,[13,14] flow sensors,[15–17] inertial sensors[18,19] and micro-heaters.[10,20] In addition, the operation of thermal-based sensors (*e.g.* thermal flow sensors and convective accelerometers) relies on the Joule heating effect, which requires a low resistivity for small supply voltage and ease of detection. Consequently, crystalline SiC is a suitable choice for such applications. This material can also be employed for thermal-based sensors integrated with on-chip electronic devices. Furthermore, the low substrate conductivity is a crucial property for the operation of such SiC thermal sensors.[10,21] However, both the vertical current leakage and the degrading electrical property of the silicon (Si) substrate at high temperatures limit the applications of 3C–SiC on Si platforms for high-temperature electronic devices.[22,23] A solution for this problem is transferring SiC onto an insulating substrate. Characterizing the thermoresistive property of the transferred SiC film is of great interest for practical applications.

Since single crystalline 3C–SiC cannot be grown on any insulating substrates, recent research has focused on transferring techniques such as Smart Cut[24] and wafer bonding,[25] to create high-quality single crystalline 3C–SiC thin films on insulating substrates. However, these techniques suffer several disadvantages such as implantation damage and a limitation of the implanted oxide layer thickness.

In this paper, we report the growth of the p-3C–SiC on Si wafer by Low-Pressure Chemical Vapour Deposition (LPCVD) and the subsequent transfer of the SiC thin film to a glass substrate using the Focused Ion Beam (FIB) technique. We characterized the thermoresistive properties of this material and observed a relatively high temperature coefficient of resistance (TCR). We also demonstrated the use of p-3C–SiC on SiO_2 as a suitable material system for high-temperature thermal-based sensors.

The LPCVD process was performed at a temperature of 1273 K to grow p-3C–SiC nanoscale thin films with a thickness of 280 nm on (100) Si substrate. Silane (SiH_4) and propylene (C_3H_6) were employed as alternating precursors. To form p-type SiC material, the trimethylaluminum [$(CH_3)_3Al$, TMAl] precursor was exploited in the *in situ* doping process. Fig. 1(a) shows the full-range of X-ray Diffraction (XRD) measurement, indicating the growth of 3C–SiC on Si. The full width at half maximum (FWHM) of approximately 0.8 degree was observed (Fig. 1(b)). Furthermore, the Transmission Electron Microscope (TEM) image (Fig. 1(c)) indicates good crystallinity of the as-grown SiC

[a]Queensland Micro- and Nanotechnology Centre, Griffith University, Brisbane, Queensland 4111, Australia. E-mail: toan.dinh@griffithuni.edu.au

[b]Department of Mechanical Engineering, University of Hyogo, Hyogo, Japan

[c]School of Engineering, Griffith University, Queensland, Australia

† Electronic supplementary information (ESI) available: The fabrication processes, experimental setup for thermoresistive characterization, the current flow in p-3C–SiC on Si, and the impact of thermoelectric effect. See DOI: 10.1039/c5ra20289b

‡ Toan Dinh and Hoang-Phuong Phan contributed equally to this work.

Published on 07 December 2015. Downloaded on 3/2/2020 4:50:36 AM.

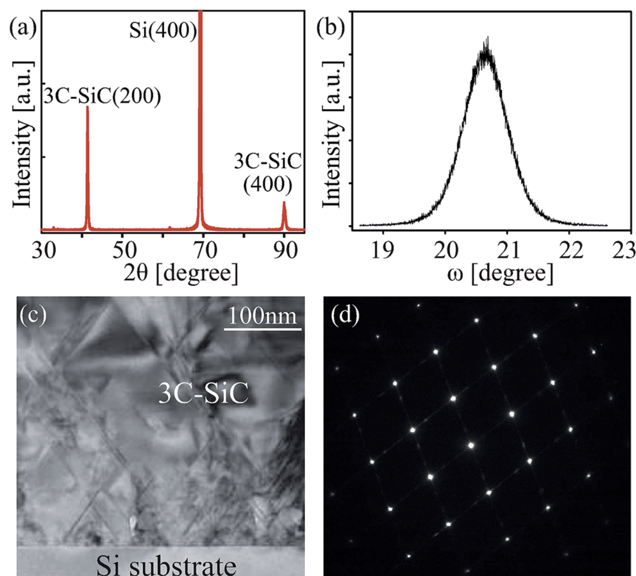

Fig. 1 Characteristics of the SiC film: (a) the XRD graph of p-3C–SiC grown on (100) Si; (b) the rocking curve scan of 3C–SiC; (c) the TEM image of 3C–SiC; (d) the SAED image of 3C–SiC. (Reproduced with permission from ref. 8. Copyright [2014], AIP Publishing LLC).

film. In addition, the selected area electron diffraction (SAED) (Fig. 1(d)) confirms the single crystalline characteristics of the as-grown SiC film.

The Hall measurement was also performed to determine the carrier concentration of the films at room temperature (~300 K). The obtained results indicate a carrier concentration of 5×10^{18} cm^{-3} for the as-grown SiC films. In addition, the resistivity of the p-3C–SiC films was measured to be approximately 0.14 Ω cm^{-1}. This resistivity is in the common range used for thermal-based sensors.[10] We also investigated the current flow in p-3C–SiC on a Si substrate as a reference (ESI†). The results indicate that p-3C–SiC on a Si substrate is not a good choice for thermal-based sensors at temperatures higher than 350 K. Therefore, we transferred the p-3C–SiC onto SiO_2 and then examined its thermoresistive property for a temperature range of 300 to 600 K, which will be presented hereafter.

We formed the I-shaped SiC resistors on the Si substrate using standard photolithography and dry etching processes[26,27] (ESI†), Fig. 2(a). Aluminum electrodes were used for making the Ohmic contacts between the SiC films and the subsequent deposited tungsten. We then released the SiC resistors from the substrate, employing an isotropic dry etching process with XeF_2 as the etching gas[28] (ESI†), Fig. 2(b). Next, we utilized FIB to remove the SiC films from the Si substrate, Fig. 2(c). A micro probe (ESI†) was then employed to transfer the SiC resistors onto a SiO_2 substrate where aluminum electrodes were readily deposited, Fig. 2(d). Finally, a tungsten layer was deposited to fix the SiC films on the SiO_2 substrate, Fig. 2(e). Fig. 2(f) shows a scanning electron microscope (SEM) image of a SiC resistor after it was transferred to the insulating substrate.

An experimental setup was established for the thermoresistive characterization of the p-3C–SiC films (ESI†).[13] Fig. 3 shows the typical current–voltage (*I–V*) curves of the p-3C–SiC

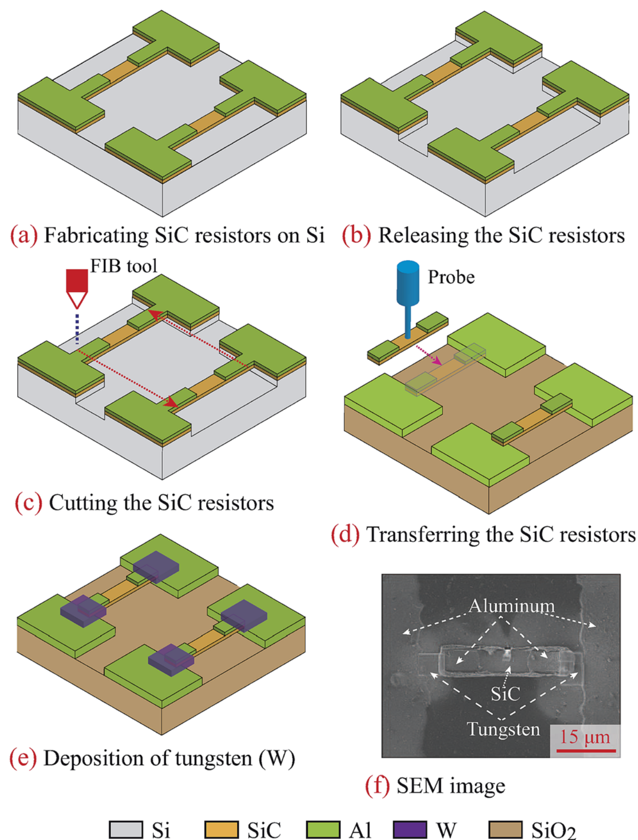

Fig. 2 Fabrication steps of p-3C–SiC on SiO_2: (a) fabrication of p-3C–SiC on Si substrates; (b) releasing the SiC structures; (c) cutting the SiC resistors using a Focused Ion Beam (FIB) method; (d) transferring the SiC onto a SiO_2 substrate; (e) deposition of tungsten (W); (f) scanning Electron Microscopy (SEM) image of p-3C–SiC on SiO_2.

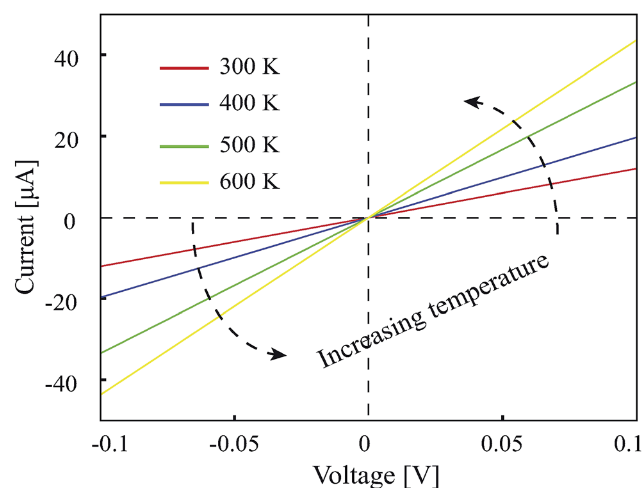

Fig. 3 The current–voltage (*I–V*) characteristic of p-3C–SiC on a SiO_2 substrate measured at different temperatures.

film at various temperatures ranging from room temperature of 300 K to 600 K. The applied voltage varied from −0.1 V to 0.1 V. The *I–V* curves show that a good contact between the aluminum electrodes and the p-type 3C–SiC was maintained in the whole

 This journal is © The Royal Society of Chemistry 2015

Published on 07 December 2015. Downloaded on 3/2/2020 4:50:36 AM.

temperature range. The *I–V* data also indicate that the conduction of SiC is thermally activated, because impurities are ionized with increasing temperature. In addition, the thermoelectric effect of the Al–W junction can be neglected because the temperature distribution of the device is expected to be uniform (ESI†). This assumption is experimentally supported by the fact that the linear *I–V* curves pass through the origin at elevated temperatures (Fig. 3).

Fig. 4(a) shows the resistance values derived from the *I–V* data. The resistance decreases significantly with increasing temperature (*e.g.* up to 80% at 600 K). As a result, the measured temperature coefficient of resistance (TCR) varies from −2400 ppm K^{-1} to −5500 ppm K^{-1}, Fig. 4(b). This TCR is comparable to that of other thermal sensing materials such as platinum (3920 ppm K^{-1}).

The p-type 3C–SiC doped with a concentration of 5×10^{18} cm^{-3} possesses sensitive ionization characteristics with increasing temperature, evident through the significant increase of its conductivity. We hypothesise that the free hole concentration (n) increases with increasing temperature, and remains constant once the impurities are fully ionized. Therefore, the absolute TCR is large near room temperature and decreases with increasing temperature as a result of the decrease in the hole mobility. The temperature dependence of hole concentration in p-3C–SiC can be expressed as:[29,30]

$$n \sim T^{3/2} \exp\left(-\frac{E_a}{kT}\right) \quad (1)$$

where E_a is the activation energy of the acceptor (hole), and k is the Boltzmann constant. In addition, the hole mobility decreases with increasing temperature and can be simply determined as:[31–33]

$$\mu \sim T^{-\alpha} \quad (2)$$

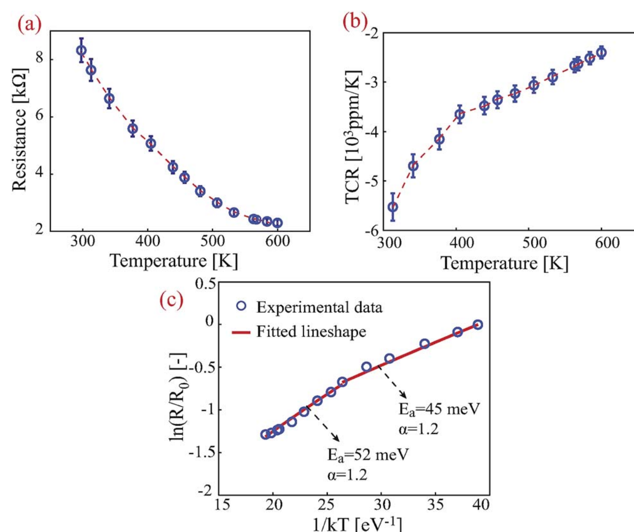

Fig. 4 Thermoresistive characteristics of the p-3C–SiC on a SiO_2 platform: (a) electrical resistance *versus* temperature (number of samples $N = 4$); (b) temperature coefficient of resistance (TCR) of the p-3C–SiC material; (c) non-linear Arrhenius plot of the p-3C–SiC thermoresistance and its fitting curves.

where α is an experimental constant. The resistivity (ρ) of the SiC films can be determined from the hole concentration (eqn (1)) and its mobility (eqn (2)) using eqn (3) as follows:

$$\rho = \frac{1}{q\mu n} \sim T^{\alpha-3/2} \exp\left(\frac{E_a}{kT}\right) \quad (3)$$

where q is the electron charge. Deducing from eqn (3), the relationship between the resistance change and the temperature can be written in the following form:

$$\ln\left(\frac{R}{R_0}\right) = \left(\alpha - \frac{3}{2}\right)\ln\left(\frac{T}{T_0}\right) + E_a\left(\frac{1}{kT} - \frac{1}{kT_0}\right) \quad (4)$$

where R_0 is the SiC resistance at the reference temperature T_0. Fig. 4(c) shows the non-linear Arrhenius plot of the p-3C–SiC and its fitted curves based on eqn (4). The hole mobility constant was found to be 1.2, and two activation energy thresholds of 45 meV and 52 meV were extracted, corresponding to temperature ranges of 300 K to approximately 450 K and 450 K to 600 K, respectively. These low activation energy thresholds were found, which are due to the fact that the doped SiC film has a large hole concentration (5×10^{18} cm^{-3}). At this concentration, the impurities are partly ionized at room temperature. Thus, the Fermi level becomes closer to the valence band of SiC. In addition, as the low activation energy thresholds of 45 meV and 52 meV were found, it is likely that the holes from the acceptor levels require a small increase in thermal energy to be activated into the top edge of the valence band. Since the energy band gap of the 3C–SiC material is approximately 2.3 eV,[34] the calculated ratio of $2E_a/E_g$ was much smaller than the utility, indicating that the Fermi level is deeply located in the lower region of the forbidden band. It is also important to note that the scattering mechanism cannot be neglected, since the phonon scattering $\mu \sim T^{-1.2}$ limits the decrease in the resistivity of the SiC film at high temperatures.

In conclusion, we investigated the thermoresistive properties of p-3C–SiC grown on Si substrate, peeled off by FIB, and subsequently transferred on to a glass substrate. We then studied the conduction mechanism of the SiC material and found two low activation energy thresholds of 45 meV and 52 meV, as well as a temperature dependent mobility of $\mu \sim T^{-1.2}$. A negative and large TCR up to −5500 ppm K^{-1} was also obtained, demonstrating the feasibility of using this material for thermal-based sensors working in high-temperature environments.

Acknowledgements

This work was performed in part at the Queensland node of the Australian National Fabrication Facility, a company established under the National Collaborative Research Infrastructure Strategy to provide nano and micro-fabrication facilities for Australia's researchers. This work has been partially supported by the Griffith University's New Researcher Grants and Australian Research Council grant LP150100153.

References

1 M. Mehregany, C. Zorman, N. Rajan and C. H. Wu, *Proc. IEEE*, 1998, **86**, 1594–1609.

Published on 07 December 2015. Downloaded on 3/2/2020 4:50:36 AM.

2 V. Cimalla, J. Pezoldt and O. Ambacher, *J. Phys. D: Appl. Phys.*, 2007, **40**, 6386.
3 H. P. Phan, D. V. Dao, K. Nakamura, S. Dimitrijev and N. T. Nguyen, *J. Microelectromech. Syst.*, 2015, **24**, 1663–1677.
4 H. P. Phan, D. V. Dao, L. Wang, T. Dinh, N. T. Nguyen, A. Qamar, P. Tanner, S. Dimitrijev and Y. Zhu, *J. Mater. Chem. C*, 2015, **3**(6), 1172.
5 A. Qamar, P. Tanner, D. V. Dao, H. P. Phan and T. Dinh, *Electron Device Lett.*, 2014, **35**, 1293–1295.
6 A. Qamar, D. V. Dao, P. Tanner, H. P. Phan, T. Dinh and S. Dimitrijev, *Appl. Phys. Express*, 2015, **8**, 061302.
7 L. Wang, S. Dimitrijev, J. Han, P. Tanner, A. Iacopi and L. Hold, *J. Cryst. Growth*, 2011, **329**, 67–70.
8 H. P. Phan, D. V. Dao, P. Tanner, L. Wang, N. T. Nguyen, Y. Zhu and S. Dimitrijev, *Appl. Phys. Lett.*, 2014, **104**, 111905.
9 H. P. Phan, P. Tanner, D. V. Dao, L. Wang, N. T. Nguyen, Y. Zhu and S. Dimitrijev, *Electron Device Lett.*, 2014, **35**, 399–401.
10 S. Noh, J. Seo and E. Lee, *Trans. Electr. Electron. Mater.*, 2009, **10**, 131–134.
11 X. Lin, S. Lin, Y. Xu, A. A. Hakro, T. Hasan, B. Zhang and H. Chen, *J. Mater. Chem. C*, 2013, **1**, 2131–2135.
12 C. Lyons, A. Friedberger, W. Welser, G. Muller, G. Krotz and R. Kassing, *IEEE Int. Conf. Micro Electro Mech. Syst., 11th*, 1998, pp. 356–360.
13 T. Dinh, D. V. Dao, H. P. Phan, L. Wang, A. Qamar, N. T. Nguyen, P. Tanner and M. Rybachuk, *Appl. Phys. Express*, 2015, **8**, 061303.
14 C. Yan, J. Wang and P. S. Lee, *ACS Nano*, 2015, **9**, 2130–2137.
15 T. Dinh, H. P. Phan, D. V. Dao, P. Woodfield, A. Qamar and N. T. Nguyen, *J. Mater. Chem. C*, 2015, **3**, 8776.
16 N. T. Nguyen, *IEEE Sens. J.*, 2005, **5**, 1224–1234.
17 W. C. Lin and M. A. Burns, *Anal. Methods*, 2015, **7**, 3981–3987.
18 V. T. Dau, D. V. Dao and S. Sugiyama, *Smart Mater. Struct.*, 2007, **16**, 2308–2314.
19 D. V. Dao, V. T. Dau, T. Shiozawa and S. Sugiyama, *J. Microelectromech. Syst.*, 2007, **16**, 950–958.
20 V. T. Dau, D. V. Dao, T. Yamada, B. T. Tung, K. Hata and S. Sugiyama, *Smart Mater. Struct.*, 2010, **19**, 075003.
21 J. T. W. Kuo, L. Yu and E. Meng, *Micromachines*, 2012, **3**, 550–573.
22 C. Dezauzier, N. Becourt, G. Arnaud, S. Contreras, J. L. Ponthenier, J. Camassel and C. Jaussaud, *Sens. Actuators, A*, 1995, **46**, 71–75.
23 F. Mailly, A. Giani, R. Bonnot, P. Temple-Boyer, F. Fascal-Delannoy, A. Foucaran and A. Boyer, *Sens. Actuators, A*, 2001, **94**, 32–38.
24 L. Di Cioccio, F. Letertre, Y. le Tiec, A. M. Papon, C. Jaussaud and M. Bruel, *Mater. Sci. Eng., B*, 1997, **46**, 349–356.
25 Q. Y. Tong, U. Gosele, C. Yuan, A. J. Steckl and M. Reiche, *J. Electrochem. Soc.*, 1995, **142**, 232–236.
26 A. Qamar, H. P. Phan, D. V. Dao, P. Tanner, T. Dinh, L. Wang and S. Dimitrijev, *Electron Device Lett.*, 2015, **36**, 708–710.
27 H. P. Phan, A. Qamar, D. V. Dao, T. Dinh, L. Wang, J. Han and N. T. Nguyen, *RSC Adv.*, 2015, **5**, 56377–56381.
28 D. Xu, B. Xiong, G. Wu, Y. Wang, X. Sun and Y. Wang, *J. Microelectromech. Syst.*, 2012, **21**, 1436–1444.
29 S. O. Kasap, Semiconductor, *Principles of Electronic Materials and Devices*, McGraw-Hill, New York, NY, 2006, p. 373.
30 S. S. Li and W. R. Thurber, *Solid-State Electron.*, 1977, **20**, 609–616.
31 S. O. Kasap, Electrical and thermal conduction in solids, *Principles of Electronic Materials and Devices*, New York, NY, McGraw-Hill, 2006, p. 113.
32 M. Roschke and F. Schwierz, *IEEE Trans. Electron Devices*, 2001, **48**, 1442–1447.
33 K. Sasaki, E. Sakuma, S. Misawa, S. Yoshida and S. Gonda, *Appl. Phys. Lett.*, 1984, **45**, 72–73.
34 R. G. Humphreys, D. Bimberg and W. J. Choyke, *Solid State Commun.*, 1981, **39**, 163.

 This journal is © The Royal Society of Chemistry 2015